ISSN 1027-4510, Journal of Surface Investigation: X-ray, Synchrotron and Neutron Techniques, 2017, Vol. 11, No. 2, pp. 443–448. © Pleiades Publishing, Ltd., 2017.
Original Russian Text © N.A. Djuzhev, M.A. Makhiboroda, R.Y. Preobrazhensky, G.D. Demin, E.E. Gusev, A.A. Dedkova, 2017, published in Poverkhnost', 2017, No. 4, pp. 64–70.

Development and Study of a Conceptual Model of an X-Ray Source with a Field Emission Cathode

N. A. Djuzhev, M. A. Makhiboroda, R. Y. Preobrazhensky*, G. D. Demin, E. E. Gusev, and A. A. Dedkova

National Research University of Electronic Technology "MIET", Moscow, 124498 Russia

**e-mail: cogtepsum@gmail.com*

Received March 9, 2016

Abstract—A conceptual model of an X-ray source based on a field emission cathode and a transmission-type target combined with a silicon X-ray window is suggested. By numerical simulation, it is shown that the proposed structure can generate a substantial emission current. It is possible to obtain a small focal spot at the target and, therefore, a high resolution. The parameters of targets providing the maximum X-ray emission intensity are determined. It is shown that effective generation is reached in a 0.25-μm-thick tungsten film and a 0.13-μm-thick molybdenum film. The transparency of a 1–2-μm-thick silicon membrane to X-rays and sufficient mechanical strength of the membrane against a pressure drop on the order of 2 atm are demonstrated, which indicates the possibility of its application as an X-ray window.

Keywords: X-ray source, field emission nanocathode, electron field emission, emission current, microelectromechanical systems, X-ray radiation, computer modeling

DOI: 10.1134/S1027451017020239

INTRODUCTION

Nowadays, in various areas of science and technology, there is an urgent need for miniature X-ray sources with low energy consumption, the ability to scan with X-rays and vary the emission frequency, and that have a short set-up time.

Such X-ray sources are needed for a wide variety of practical applications, such as medical equipment, devices for X-ray fluorescence analysis, safety and anti-terror systems. The increasing sensitivity of X-ray sensors increases the need for X-ray tubes of low and ultra-low power (a few watts) and low voltage (with a voltage on the order of 10 kV), because such an X-ray source, especially working in the pulsed mode, is virtually harmless to humans.

X-ray sources can find application in advanced analytical equipment and in the technology of nanostructures and novel materials. Using X-ray sources, it is possible to study the structure of objects and obtain their 3D images. Such radiation barely interacts with objects and, in many cases, does not require special preparation.

The use of a field emission source as an alternative to a traditional incandescent emitter is very attractive and promising for practical applications. The main advantages of a cold electron source are a result of the fundamental difference between the cold electron and thermoelectron emission processes. Electron (cold) field emission is a purely quantum effect. Electron emission does not require the expenditure of energy in the act of emission in contrast to thermal emission, which requires cathode heating. In addition, the use of a field emitter makes it possible to avoid contamination of the target surface with products of thermocathode emission, which significantly reduces the purity of vacuum and deteriorates the emission characteristics of an X-ray source in the working region of soft X-ray radiation. The field-emission current density exponentially depends on the strength of the applied electric field and can exceed a million-fold the emission current density of any form. Due to the tunneling character of emission, the spread in the emitted electron energy is several-fold narrower than in the case of thermal emission. Electron field emission should be excited at low temperatures down to absolute zero. The field emission process is practically inertialess [1].

Due to these specific features, a cold-cathode device provides lower energy consumption, higher speed, shorter preparation time, wider temperature range, and general miniaturization. However, in the context of X-ray sources, the main advantage of a nanoscale cold emitter is a narrow electron beam, which makes it possible to obtain small focal spots on the target. Depending on a particular application, the role of an electron source can be played by a single-emission cathode working in tandem with the electron-optical system and providing a sub-millimeter focal spot; it can also be an array of such emitters,

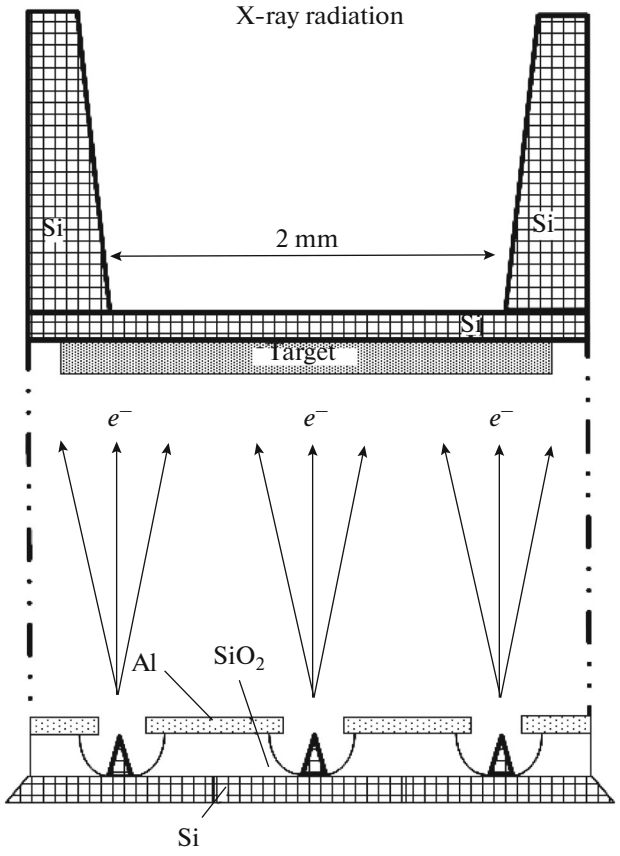

Fig 1. Conceptual model of an X-ray source.

which make it possible to attain high values of the total cathode current [2].

Another step toward the miniaturization of an X-ray source is the use of a transmission-type target combined with an output X-ray window. Such a target consists of a thin-film anode in which X-ray radiation is produced under the action of an electron beam. The film is applied onto the inner surface of a window made of a material transparent to X-rays and which provides the output of radiation from the device. Nowadays, X-ray windows are usually made of beryllium plates with a thickness of about 150 μm. However, the high price and low production efficiency of the fabrication of beryllium X-ray windows stimulates the search for alternative variants. Such an alternative may be a transmission-type target formed on a silicon membrane by the microelectromechanical systems (MEMS) technology.

Here, we present the concept of an X-ray source consisting of an array of field-emission cathode nodes separated by a free-space gap from a thin-film metallic transmission-type target formed on a silicon membrane which plays the role of an X-ray window. Mathematical models of the nanoscale cathode, thin-film transmission-type target, and a silicon X-ray window are developed. Simulation using the COMSOL Multiphysics software package [3] is performed, and results important for the further development of this promising project are obtained.

1. CONCEPTUAL MODEL OF AN X-RAY SOURCE

In the proposed concept of an X-ray source, the role of the cathode is played by an array of field emission tip emitters with a tip rounding radius of a few nanometers. The control electrode, common for the entire array, is made in the form of a thin metal film with an aperture in front of each emitter. The control electrode is insulated from the cathode by a dielectric layer. Such a layer of field emission nodes is made from silicon by the MEMS technology [4]. The X-ray window is a square silicon membrane formed on a plate by anisotropic etching, the side length being 2 mm. The role of the transmission-type target was played by a metal film applied onto the inner surface of the membrane. A schematic of the model is shown in Fig. 1.

Using mathematical modeling, in the framework of the proposed concept, we had to solve the following basic problems: determination of the emission characteristics of a single cathode node with the given configuration and number of cathode nodes in the array necessary to provide the desired total emission current; calculation of the trajectories of emitted electrons and focal spot on the target; determination of the thickness of the transmission-type target as a function of the chosen material, the intensity of generated characteristic radiation, and optimal parameters of the silicon X-ray window, at which—in combination with the chosen X-ray window—minimum X-ray absorption with sufficient mechanical strength are reached.

2. DEVELOPMENT AND ANALYSIS OF THE MATHEMATICAL MODEL OF A NANOCATHODE

One of the main elements of a scanning X-ray source is a nanocathode produced in the form of a needle with a tip rounding radius of 10 nm. The most important requirement to a nanocathode is a sufficient emission current generated under the action of an external electric field. In addition, the linear sizes and configuration of a nanocathode must give the possibility of forming an array of such structures in order to increase the total emission current in the device (the target value was 75 μA). Other important characteristics of a nanocathode are the character of the trajectories of emitted electrons and the diameter of the resulting electron beam. These parameters of the device greatly depend on the configuration of the electric field near the tip of the nanocathode [5].

The suggested nanocathode form is shown in Fig. 2. The main elements are the substrate with a tip formed on it, an insulating dielectric layer, and the metal film

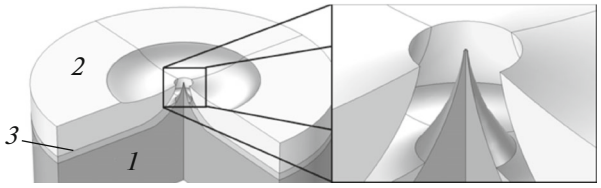

Fig. 2. Geometry of a nanocathode: (*1*) silicon (substrate); (*2*) metallic extraction electrode; (*3*) dielectric insulating layer.

of the extraction electrode. The geometrical sizes of the cathode, presented in Table 1, were chosen in accordance with the aforementioned requirements.

The voltages applied to the system vary as follows: the potential difference at the extraction electrode varies in the range of 100–150 V, and the voltage at the transmission-type target varies in the range of 0–40 kV. The electric-field distribution in the system was simulated using the COMSOL Multiphysics software package for interdisciplinary analysis [3].

The simulated electric-field distribution on the tip surface was used to calculate the emission current from the Fowler–Nordheim equation [6]:

$$j = \frac{eF^2}{4\pi^2\hbar U_0}\sqrt{\frac{\mu}{U_0-\mu}}\exp\left[-\left(\frac{4\sqrt{2m}}{3F\hbar}\right)(U_0-\mu)^{\frac{3}{2}}\right],$$

where F is the electrostatic force defined as a product of the elementary charge e by the electric-field strength E, μ is the Fermi level (in the given case, for highly alloyed silicon, the value of 2.12 eV was taken), U_0 is the potential barrier height (6.27 eV), and m is the electron mass. The electric-field strength and emission current distributions are shown in Figs. 3a and 3b. Figure 3c shows the emission current as a function of the voltage at the extraction electrode and the target.

We can see that an appreciable current arises when the voltage at the extraction electrode is 100 V and reaches values of about 90 nA at a voltage of 150 V. Therefore, to provide a total emission current of 75 μm, an array of ~850 nanocathodes is needed. Since the linear sizes of the nanocathodes do not exceed 10 μm, the arrangement of such a number of nanocathodes on a small area is technically feasible. The trajectories of emission electrodes are calculated from the electric-field distribution by the formula

$$d\left(m_p v\right)/dt = F = eZE,$$

where m_p is the particle mass, v is the particle velocity, F is the electrostatic force, e is the elementary charge, Z is the particle charge number, and E is the electric-field strength. Calculation was performed using the COMSOL Multiphysics software package. The initial particle distribution density over the cathode surface is specified to be proportional to the emission current calculated above. The resulting trajectories are shown in Fig. 4. The radius of the electron spot on the target

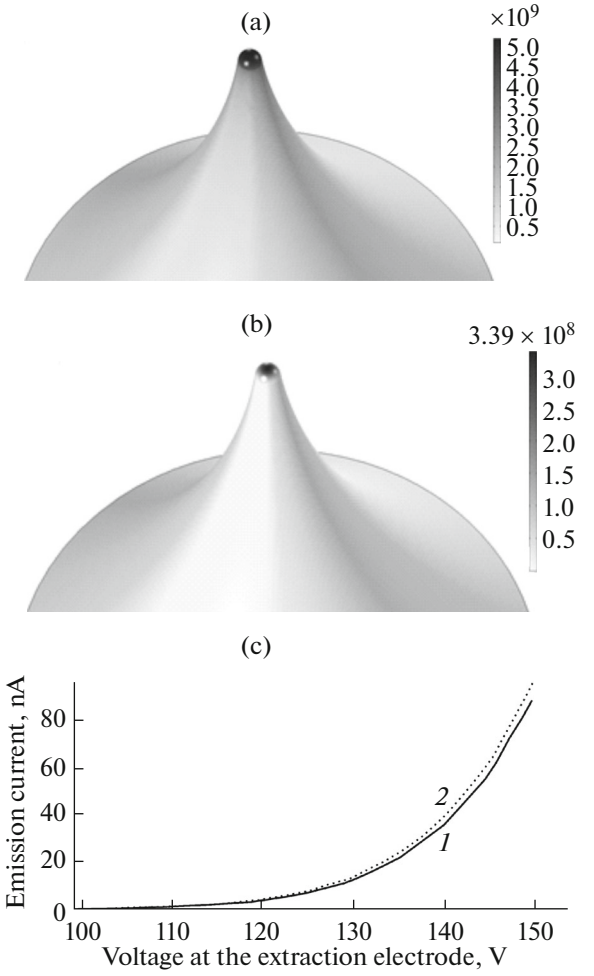

Fig. 3. (a) Electric-field strength and (b) emission current density distributions over the nanocathode tip surface. (c) Emission current vs. the voltage at the electrodes, the voltage at the target being (*1*) 0 and (*2*) 30 kV.

consisting of an array of emitters was approximately 300 μm.

Thus, the simulation of the most important parameters of a nanocathode gave results satisfying the concept's requirements to this element of the field emission node.

Table 1. Basic dimensions of a nanocathode element

Parameter	Value
Tip rounding radius	10 nm
Aperture radius in the extraction electrode	4.5 μm
Needle height	1 μm
Dielectric thickness	0.2 μm
Electrode film thickness	0.9 μm
Distance to target	5 mm

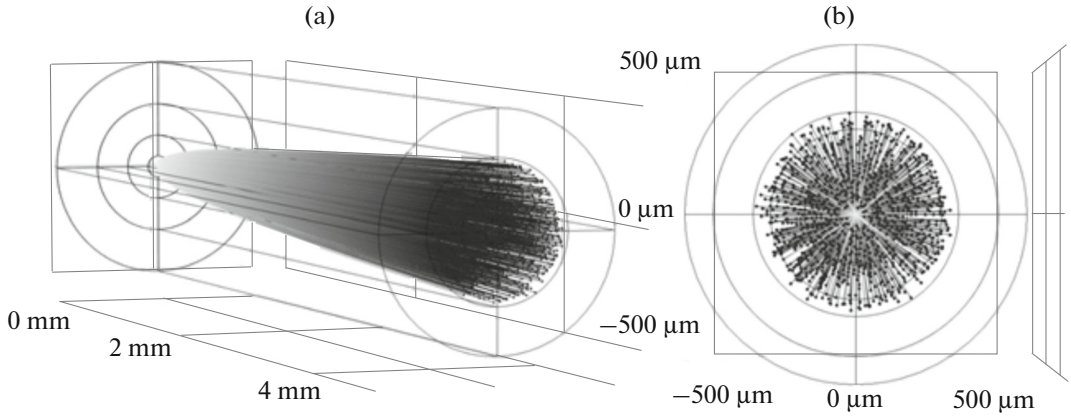

Fig. 4. Trajectories of emitted electrons in an electron-beam tube with a field emission nanocathode: (a) top and (b) front view.

3. DEVELOPMENT AND ANALYSIS OF A MATHEMATICAL MODEL OF A TRANSMISSION-TYPE TARGET

The transmission-type target of an X-ray node consists of a metal film serving as a generator of radiation and a silicon membrane transparent to X-rays, onto which the target is fixed. The silicon membrane must stand a pressure difference of at least 1 atm [7]. Correspondingly, it is necessary to determine the thickness of the metallic walls necessary for X-ray generation from the rear side of the target and the thickness of the silicon membrane providing its transparency to X-rays and high mechanical strength.

The materials chosen for the target were W ($Z = 74$) and Mo ($Z = 42$). Using the Win X-Ray [8] program, the trajectories of electrons penetrating the target material at a beam energy of 40 keV were calculated by the Monte-Carlo method. At this energy, W generates radiation with the L_α, $L_{\beta1}$, $L_{\beta2}$, L_γ, and M_α transitions, and Mo generates radiation with the $K_{\alpha1}$, $K_{\alpha2}$, $K_{\beta1}$, $K_{\beta2}$, L_α, $L_{\beta1}$, $L_{\beta2}$, and L_γ transitions. In addition, using the Win X-Ray program, the values of the characteristic intensity $\varphi(\rho z)$ were calculated for different target-film thicknesses. These calculations show that the maximum intensity of X-ray radiation emitted from the film is reached at the thicknesses presented in Table 2. The intensity distribution for different film thicknesses is shown in Fig. 5. We can see that, for efficient X-ray generation, either a 0.13-μm-thick tungsten film or 0.25-μm-thick molybdenum film is needed.

For the transparent silicon membrane, a small drop in the X-ray intensity passing through it is extremely important. This quantity is usually calculated from the Beer– Lambert–Bouguer law [9]:

$$I = I_0 \exp(-\mu d),$$

where I is the radiation intensity after passing through matter, I_0 is its initial intensity, d is the absorber's thickness, and μ is the damping coefficient.

Table 3 presents the thicknesses of a silicon membrane for which the radiation intensity drop is equivalent to the intensity drop in a 150-μm-thick beryllium membrane, transparent to X-rays (at present, beryllium is the material most widely used to produce X-ray

Table 2. Thickness of the anode film for maximum-intensity X-ray generation

Anode material	Tungsten							
Type of radiation	L_α		M_α			$L_{\beta1}$	$L_{\beta2}$	L_γ
Thickness d, nm	130		40			122	147	132
Anode material	Molybdenum							
Type of radiation	$K_{\alpha1}$	$K_{\alpha2}$	$K_{\beta1}$	$K_{\beta2}$	L_α	$L_{\beta1}$	$L_{\beta2}$	L_γ
Thickness d, nm	245		248	243	246	239	245	101

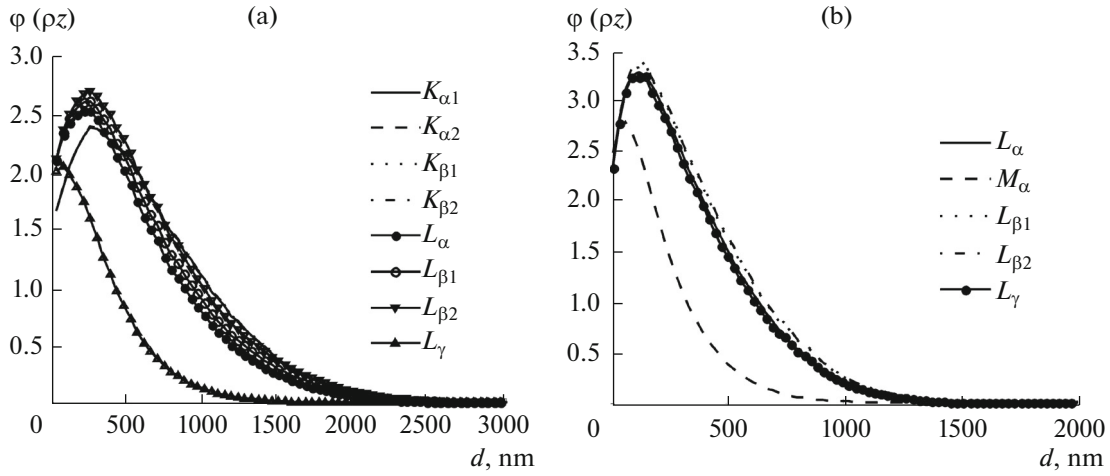

Fig. 5. Characteristic intensity vs. the thickness of (a) molybdenum and (b) tungsten target film.

widows). Table 4 presents the calculated X-ray intensities in a 1-μm-thick silicon membrane. From the results presented in Tables 3 and 4, we can conclude that the required transparency of silicon can be reached with a membrane having an average thickness on the order of 1–2 μm. Experimental measurements have shown that a silicon membrane with a thickness on the order of 1 μm and dimensions of 1 × 1 mm withstands excessive pressures above 2 atm. Thus, a silicon membrane with a thickness of 1 μm provides not only sufficient transparency to X-ray radiation generated by targets of practically all types but also the necessary mechanical strength. It follows from [9] that a transparency coefficient of greater than 0.5 for a 1-μm-

Table 3. Calculated thickness of a silicon membrane for which the radiation intensity drop is equivalent to that for a 150-μm-thick beryllium membrane, transparent to X-rays

Membrane material		Be		X-ray intensity drop I/I_0	Si	
density ρ, g/cm^3		1.848			2.33	
type of radiation	λ, Å	damping factor μ, m^{-1}	thickness, μm		damping factor μ, m^{-1}	thickness, μm
MoL_{α}	5.414	9062.897	150	0.257	461906.566	2.943
Mo$L_{\beta 1}$	5.177	7887.5502		0.306	412129.804	2.871
Mo$L_{\beta 2}$	4.923	6747.912		0.363	362013.228	2.796
MoL_{γ}	4.726	5945.339		0.410	325494.340	2.740
Mo$K_{\alpha 1}$	0.709	39.522		0.994	1433.640	4.135
Mo$K_{\alpha 2}$	0.714	39.795		0.994	1463.820	4.077
Mo$K_{\beta 1}$	0.632	35.938		0.995	1020.093	5.503
Mo$K_{\beta 2}$	0.633	35.977		0.995	1024.872	5.529
WL_{α}	1.487	168.675		0.975	12732.300	1.987
W$L_{\beta 1}$	1.245	105.304		0.984	7570.596	2.086
W$L_{\beta 2}$	1.099	78.593		0.988	5245.021	2.248
WL_{γ}	6.992	19888.861		0.056	77383.800	37.179
WM_{α}	1.282	113.323		0.983	8249.940	2.060

Table 4. Calculated X-ray radiation intensity in a 1-μm-thick silicon membrane

Type of radiation	λ, Å	X-ray radiation intensity drop I/I_0
MoL_α	5.414	0.630
Mo$L_{\beta1}$	5.177	0.662
Mo$L_{\beta2}$	4.923	0.696
MoL_γ	4.726	0.722
Mo$K_{\alpha1}$	0.709	0.998
Mo$K_{\alpha2}$	0.714	0.998
Mo$K_{\beta1}$	0.632	0.999
Mo$K_{\beta2}$	0.633	0.999
WL_α	1.487	0.987
W$L_{\beta1}$	1.245	0.992
W$L_{\beta2}$	1.099	0.995
WL_γ	6.992	0.925
WM_α	1.282	0.992

thick silicon membrane is preserved up to X-ray wavelengths of 1.6 nm.

CONCLUSIONS

In the framework of the proposed conceptual model of an X-ray source, mathematical models of a nanocathode, a thin-film transmission-type target, and a silicon X-ray window have been developed. Mathematical simulation has been performed, which showed the theoretical efficiency of the concept suggested. It has been established that an emission current of 75 μA is reached using an array of 850 nanocathodes. In this case, the voltage at the control electrode does not exceed 150 V and the diameter of the focal spot on the target situated at a distance of 5 mm is no higher than 500 μm. The operation of a transmission-type target aligned with a silicon X-ray window has been simulated. It has been shown that a 1-μm-thick silicon membrane is transparent to X-ray radiation with a wavelength of up to 1.6 nm and provides sufficient mechanical strength at a pressure difference on the order of 2 atm.

In conclusion, it should be noted that the conceptual model presented in this work is greatly simplified and disregards a number of important physical processes the most important of which are target heating and heat abstraction by the membrane. At the same time, it is the use of field emission cathodes that opens the possibility for an X-ray source to work in the pulsed mode, which—in combination with a small focal-spot size—offsets target heating, making it not so critical. Nevertheless, with further development of the model, attention will be paid to calculating thermal processes both near cold cathodes and in the region of the X-ray window [10]. Another way to perfect the concept would be the introduction of electron optics to control the electron beam. The combination of a field emission cathode with a narrow electron beam, electron optics, and a transmission-type target aligned with a silicon X-ray window opens up the possibility of creating a new class of devices: scanning devices and multifrequency microfocus X-ray sources.

ACKNOWLEDGMENTS

This work was carried out using equipment of the Multi-Access Center "Microsystems Technics and Electronic Component Base" of the National Research University of Electronic Technology and was supported by the Ministry of Education and Science of the Russian Federation in the framework of the Federal Targeted Program "Research and Development in Priority Directions of Development of the Scientific and Technological Complex of Russia for 2014–2020" (state contract no. 14.578.21.0001, agreement id. RFMEFI57814X0001).

REFERENCES

1. G. N. Fursei, Sorovskii Obraz. Zh. **6** (11), 96 (2000).
2. P. R. Shwoebel, C. A. Spindt, and C. E. Holland, J. Vac. Sci. Technol., B: Microelectron. Nanometer Struct. **23**, 691 (2005).
3. http://www.comsol.com/.
4. N. A. Dyuzhev, M. A. Makhiboroda, E. E. Gusev, T. A. Gryazneva, and G. D. Demin, *Collection of Scientific Works. Promising Micro- and Nanoelectronic Systems: Design Problem,* Ed. by A. L. Stempkovskii (Institute for Design Problems in Microelectronics Russ. Acad. Sci., Moscow, 2016), Part 4, p. 37 [in Russian].
5. B. Lepetit, D. Lemoine, and M. Márquez-Mijares, J. Appl. Phys. **120**, 085105 (2016).
6. R. H. Fowler and L. Nordheim, Proc. R. Soc. London, Ser. A **119** (781), 173 (1928).
7. N. A. Dyuzhev, A. A. Dedkova, E. E. Gusev, and A. V. Novak, Izv. Vyssh. Uchebn. Zaved., Elektron. **21** (4), 367 (2016).
8. H. Demers, P. Horny, R. Gauvin, and E. Lifshin, Microsc. Microanal. **8** (S2), 1498 (2002).
9. J. A. van Bokhoven and C. Lamberti, *X-Ray Absorption and X-Ray Emission Spectroscopy: Theory and Applications* (John Wiley & Sons, Chichester, 2016).
10. N. A. Djuzhev, M. A. Makhiboroda, V. I. Kretov, M. N. Churilin, and V. Yu. Rudnev, Russ. Microelectron. **41** (7), 387 (2012).

Translated by E. Chernokozhin